Two new quinoline-based regenerable fluorescent probes with AIE characteristics for the selective recognition of Cu^{2+} in aqueous solution and test strips

Jingwen Xiong [a], Zongzhi Li [a], Jihua Tan [a], Shaomin Ji [a,*], Jianwei Sun[b], Xianwei Li [a], Yanping Huo [a,*]

[a] *School of Chemical Engineering and Light Industry, Guangdong University of Technology, Guangzhou 510006, China*

[b] *Department of Chemistry, The Hong Kong University of Science and Technology, Clear Water Bay, Kowloon, Hong Kong, China*

*Corresponding authors. Tel.: +86 20 39322236; Fax: +86 20 39322235; Mobile: +86 13798135622 (Y. Huo).

E-mail addresses: yphuo@gdut.edu.cn (Y. Huo), smji@gdut.edu.cn (S. Ji).

Materials and apparatus

The compound 2-chloro-N-(quinolin-8-yl)acetamide (***I***) was prepared according to the literature. 8-aminoquinoline, chloroacetyl chloride, bromotriphenylethylene were obtained from Aladdin Chemistry Co., Ltd. 4-Formylphenylboronic acid and 8-hydroxyquinaldine were purchased from Energy Chemical Co. Ltd. The metal ion aqueous solutions used in this work (Ag^{+}, Al^{3+}, Ca^{2+}, Cd^{2+}, Co^{2+}, Cu^{2+}, Fe^{2+}, Fe^{3+}, Hg^{2+}, K^{+}, Li^{+}, Mg^{2+}, Na^{+}, Ni^{2+} and Zn^{2+}) were prepared from their chloride or nitrate salts. All the metal salts were purchased from Sinopharm Chemical Reagent Beijing Co. Ltd. Other materials were of analytical grade and used directly without further purification.

NMR spectra were conducted on Bruker AVANCE III 400 MHz and 600 MHz Superconducting Fourier in chloroform-d or DMSO-d_6 with tetramethylsilane as internal reference. PXRD data were collected on a DMAX2500 diffractometer using Cu Ka radiation. The calculated PXRD patterns were produced using the SHELXTL-XPOW program and single crystal reflection data. UV-vis absorption spectra were

obtained using the UV-vis absorption spectrometer of Ocean Optics. Fluorescence spectra were recorded with HORIBA FluoroMax-4 fluorescence spectrometer and Ocean Optics fluorescence spectrometer. All pH measurements were performed with a pHS-3C pH meter (Shanghai Precision & Scientific instrument Co., LTD., Shanghai, China). Time-resolved fluorescence spectra were measured at FLS980 (Edinburgh Instruments, England). Mass spectra (ESI) were performed on a Matrix-Assisted Laser Desorption/ Ionization Time of Flight Mass Spectrometry (MALDI-TOF-MS) and a Finnigan LCQ mass spectrometer using dichloromethanemethanol as mobile phase.

Synthesis and characterization of probe *1* and *2*

Preparation of 2-chloro-N-(quinolin-8-yl)acetamide ***(Ⅰ)***. Chloroacetyl chloride (2.7 mL) was dissolved in chloroform (2.5 mL). It was added dropwise to the solution of 8-aminoquinoline (1.44 g, 10 mmol) and triethylamine (1.5 mL) in chloroform (5.0 mL) within 1 h. After being stirred for 2 h at room temperature, the mixture was extracted 2 or 3 times with dichloromethane and then removed under reduced pressure to obtain a white solid. The white solid was purified by silica gel column chromatography, eluted with dichloromethane, to afford ***Ⅰ***. Yield: 1.38 g (62%).

^{1}H NMR (400 MHz, chloroform-d) δ 10.92 (s, 1H), 8.88 (d, J = 4.1 Hz, 1H), 8.76 (d, J = 4.1 Hz, 1H), 8.21 (d, J = 8.3 Hz, 1H), 7.58 (d, J = 6.8 Hz, 2H), 7.50 (d, J = 12.5 Hz, 1H), 4.33 (s, 2H).

Preparation of 4-(1,2,2-triphenylvinyl)benzaldehyde ***(Ⅱ)***. Bromotriphenylethylene (1.68 g, 5 mmol), 4-formylphenylboronic acid (0.97 g, 6.5 mmol), K_2CO_3 (2.76 g, 20 mmol) and Pd(dppf)Cl_2 (0.04 g, 0.05 mmol) were mixed with CH_3Ph-CH_3OH (25:25, v/v). The mixture was stirred for 16 h under N_2 at 75℃. After that, the mixture was cooled to room temperature and extracted for 2 or 3 times with dichloromethane. The organic mixture was evaporated under reduced pressure to obtain a raw product of Compound ***Ⅱ***. Finally, the raw product was purified by silica gel column chromatography using ethyl acetate/n-hexane (1:10, v/v) as the eluent to

afford compound ***II***. Yield: 1.62 g (89%).

^{1}H NMR (400 MHz, chloroform-d) δ 9.90 (s, 1H), 7.61 (d, *J* = 8.0 Hz, 2H), 7.19 (d, *J* = 8.0 Hz, 2H), 7.16 - 7.07 (m, 9H), 7.07 - 6.96 (m, 6H).

Preparation of (*E*)-2-(4-(1,2,2-triphenylvinyl)styryl)quinolin-8-yl acetate ***(III)***. Compound ***II*** (1.08 g, 3 mmol) and 8-hydroxyquinaldine (0.72 g, 4.5 mmol) were added to acetic anhydride (5 mL). Under N_2, the mixture was stirred for 40 h at 140℃. Precipitation occurred during the reaction progress. At the end of reaction, the mixture was cooled to room temperature and then washed it three times with water. Eventually, compound ***III*** was obtained after vacuum drying. Yield: 1.17 g (72%).

Preparation of (*E*)-2-(4-(1,2,2-triphenylvinyl)styryl)quinolin-8-ol ***(IV)***. Compound ***III*** (1.08 g, 2 mmol) was added to pyridine (10 mL). After being stirred for 30 min under N_2 at 135℃, H_2O (5 mL) was added to the mixture, which was kept stirring for 5 h under the same condition. At the end of reaction, the mixture was added to H_2O (50 mL) to obtain a solid. The solid was washed three times with water (100mL). Eventually, the raw product was purified by silica gel column chromatography using ethyl acetate/n-hexane (1:30, v/v) as the eluent to afford compound ***IV***. Yield: 0.70 g (70%).

^{1}H NMR (400 MHz, DMSO-d_6) δ 9.51 (s, 1H), 8.26 (d, *J* = 8.6 Hz, 1H), 8.00 (d, *J* = 16.2 Hz, 1H), 7.73 (d, *J* = 8.6 Hz, 1H), 7.47 (d, *J* = 8.1 Hz, 2H), 7.43 - 7.30 (m, 3H), 7.24 - 7.06 (m, 10H), 7.00 (dd, *J* = 15.2, 7.2 Hz, 8H).

Preparation of (*E*)-2-(2-(anthracen-9-yl)vinyl)quinolin-8-ol ***(VI)***. 9-Anthracenecarboxaldehyde (1.03 g, 5 mmol) and 8-hydroxyquinaldine (0.96 g, 6 mmol) were added to acetic anhydride (5 mL). The mixture was stirred for 40 h at 140℃. At the end of reaction, the mixture was cooled to room temperature and washed with water, and dried in vacuo to give brown viscous solid. After then, the brown viscous solid obtained in the previous step was added to pyridine (20 mL). After being stirred for 30 min at 130℃, H_2O (10 mL) was added to the mixture, and

then it was stirred for 8 h under the same condition. After the end of reaction, the mixture was added to H_2O (50 mL) to give a solid. The solid was washed three times with water (100 mL). Eventually, to purify the raw product by silica gel column chromatography using dichloromethane / petroleum ether (1:9, v/v) as the eluent to afford compound ***VI***. Yield: 1.25 g (72%).

^{1}H NMR (400 MHz, DMSO) δ 9.78 (s, 1H), 9.09 (d, J = 16.4 Hz, 1H), 8.63 (s, 1H), 8.52- 8.44 (m, 2H), 8.39 (d, J = 8.5 Hz, 1H), 8.18 - 8.12 (m, 2H), 7.99 (d, J = 8.5 Hz, 1H), 7.63 - 7.53 (m, 4H), 7.49 - 7.39 (m, 2H), 7.27 (d, J = 16.4 Hz, 1H), 7.14 (dt, J = 9.8, 4.9 Hz, 1H).

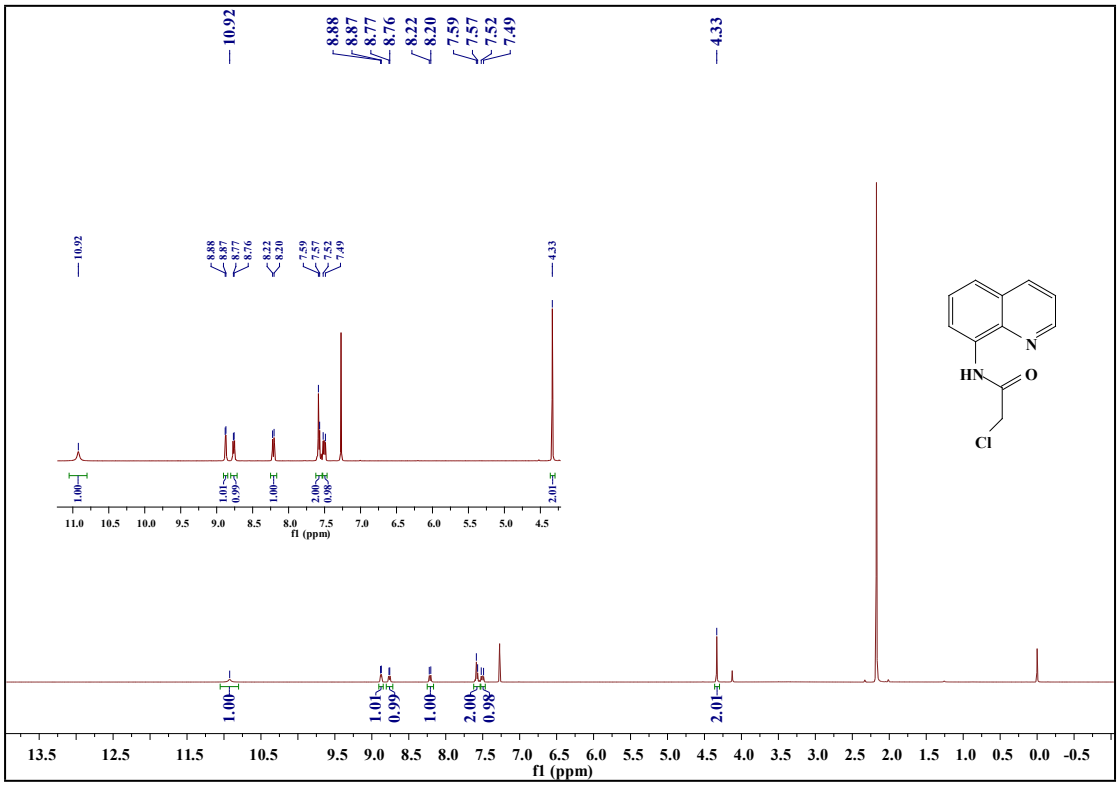

Fig.S1. ^{1}H NMR spectrum of 2-chloro-N-(quinolin-8-yl)acetamide (Chloroform-d)

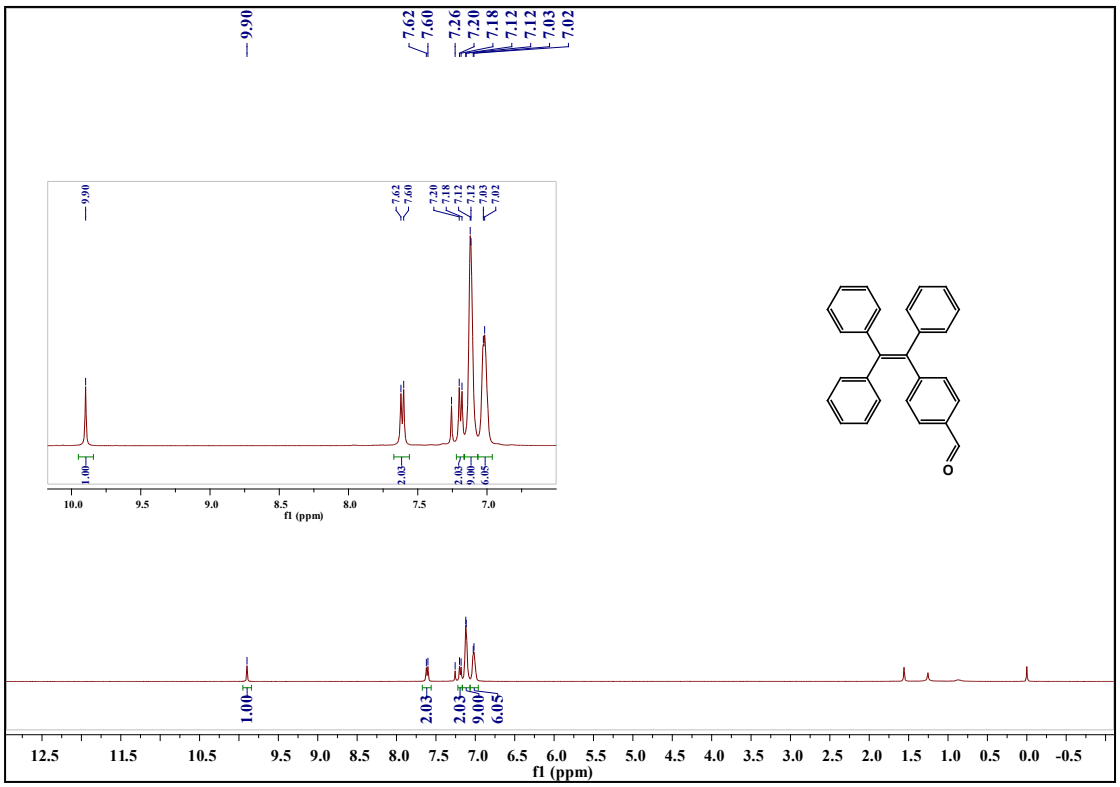

Fig.S2. ^{1}H NMR spectrum of 4-(1,2,2-triphenylvinyl)benzaldehyde (Chloroform-d)

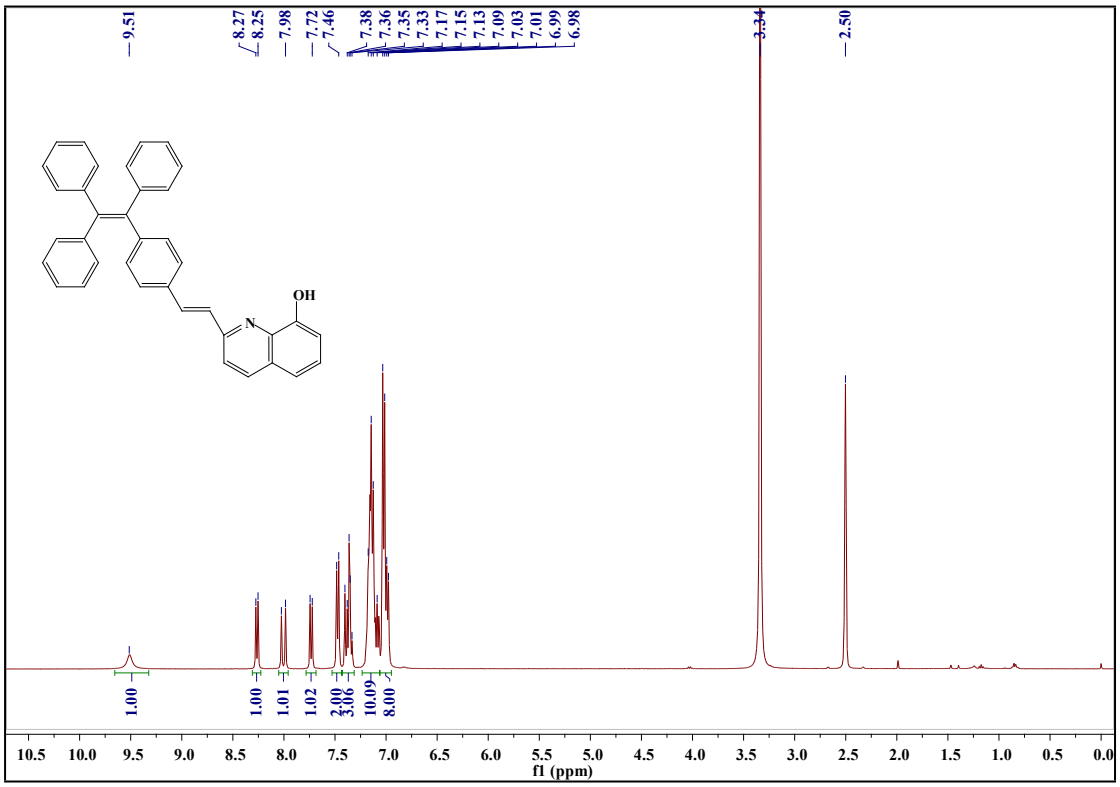

Fig.S3. ^{1}H NMR spectrum of (E)-2-(4-(1,2,2-triphenylvinyl)styryl)quinolin-8-ol (DMSO-d_6)

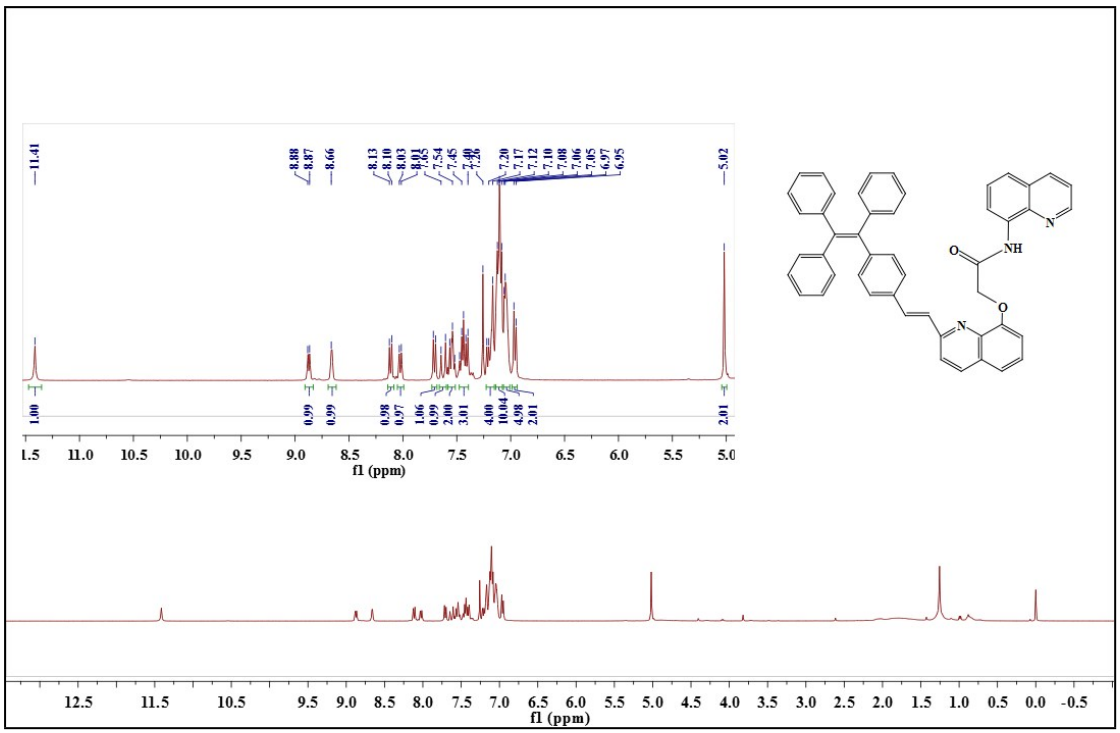

Fig.S4. ^{1}H NMR spectrum of probe ***1*** (Chloroform-d)

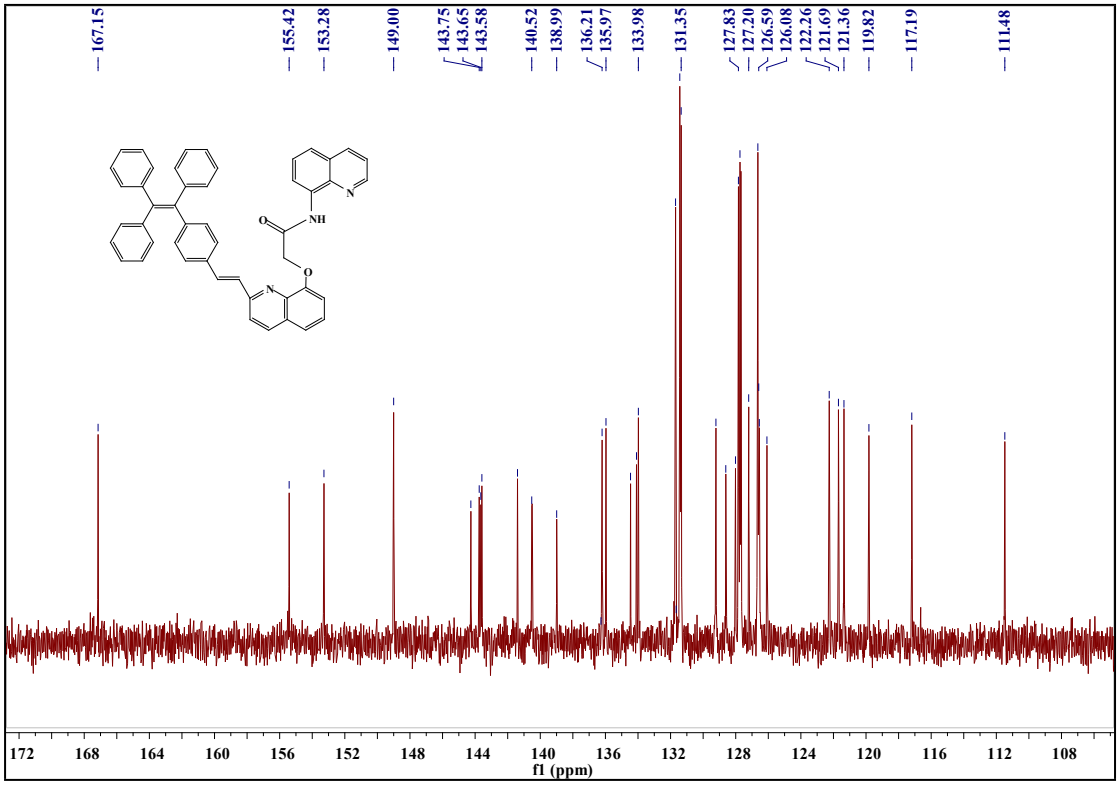

Fig.S5. ^{13}C NMR spectrum of probe ***1*** (Chloroform-d)

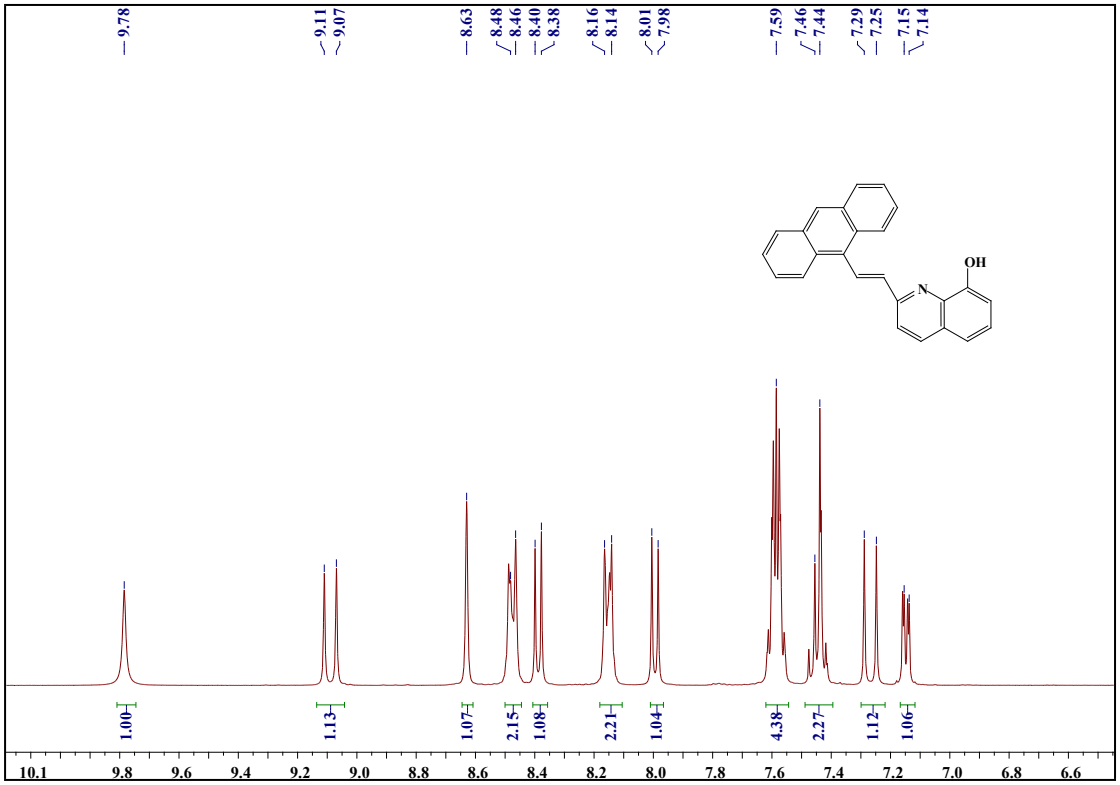

Fig.S6. ^{1}H NMR spectrum of (E)-2-(2-(anthracen-9-yl)vinyl)quinolin-8-ol ***(VI)***

(DMSO-d_6)

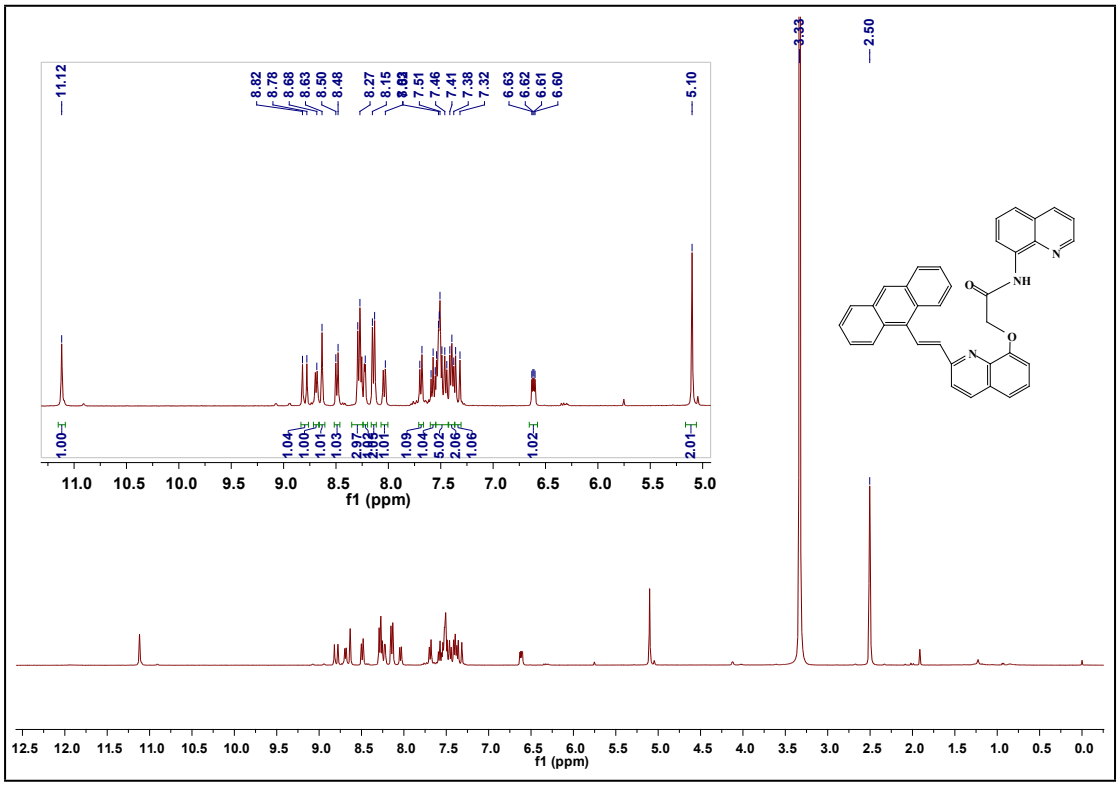

Fig.S7. ^{1}H NMR spectrum of probe ***2*** (DMSO-d_6)

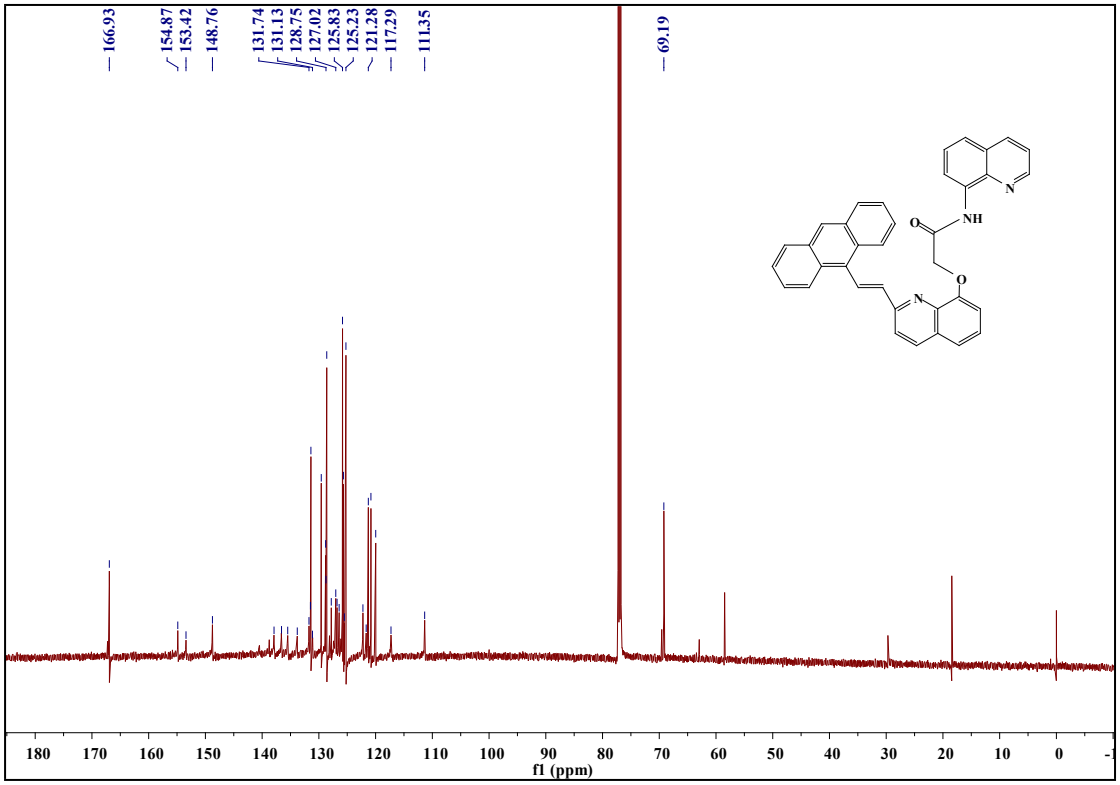

Fig.S8. ^{13}C NMR spectrum of probe ***2*** (Chloroform-d)

A)

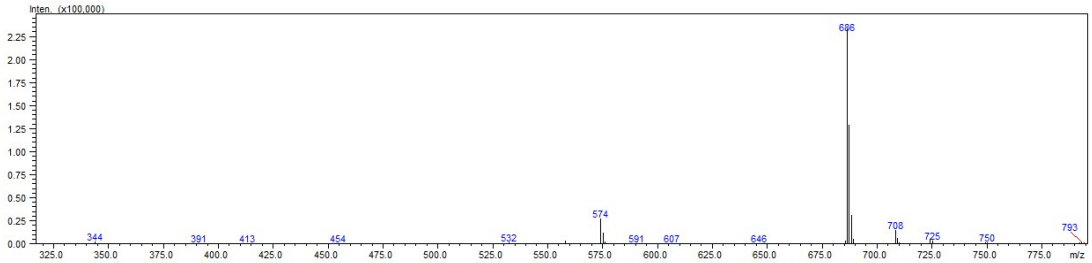

B)

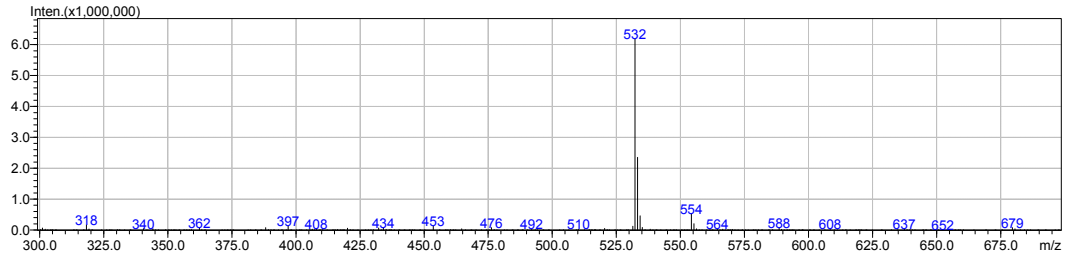

Fig.S9. (A) The MS spectrum of probe ***1*** in CH_3OH. (B) The MS spectrum of probe ***2*** in CH_3OH.

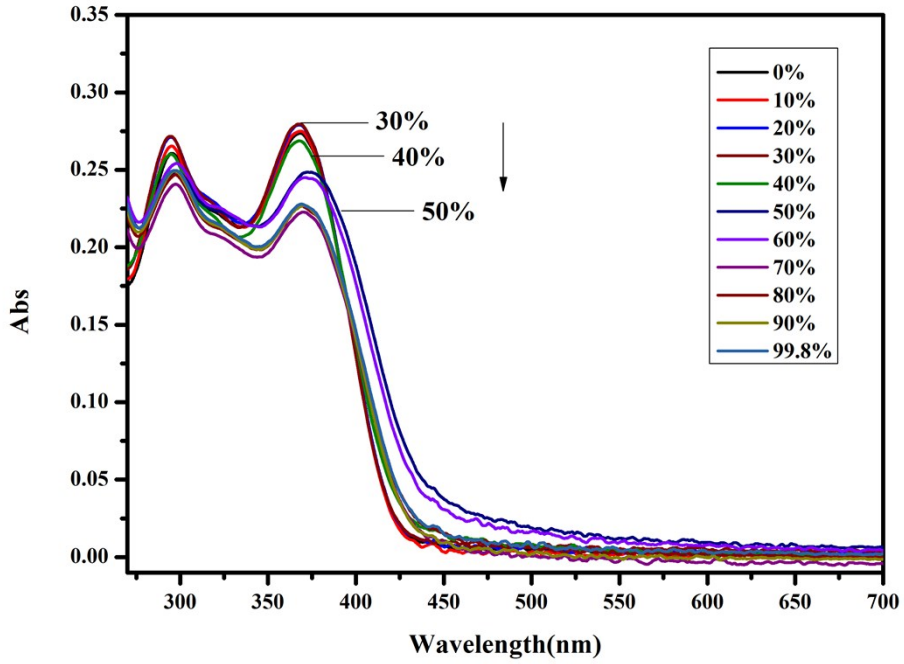

Fig.S10. UV-vis absorption spectra of ***1*** in different ratios of DMSO/H_2O.

Concentration: 10 μM.

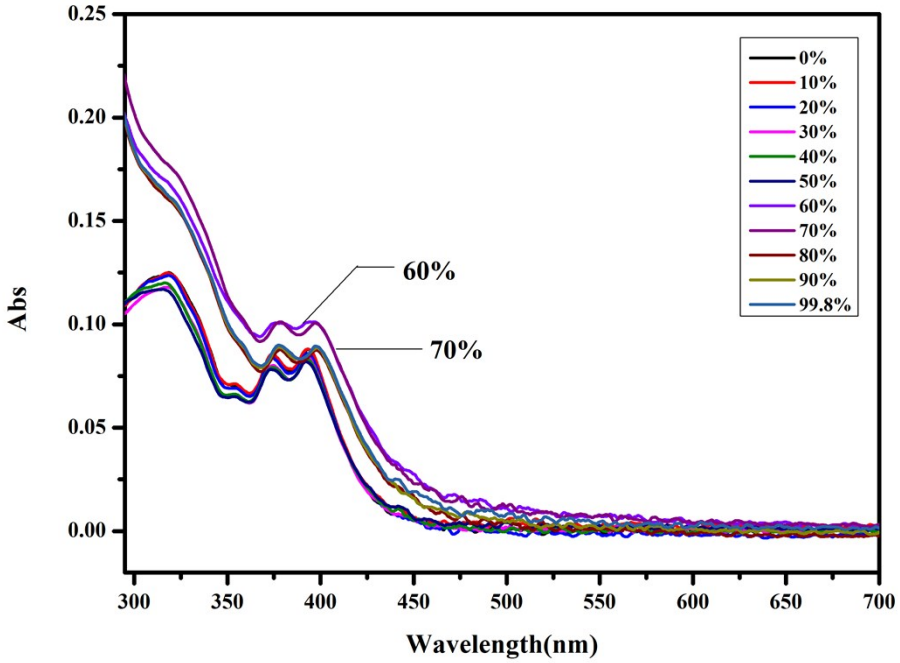

Fig.S11. UV-vis absorption spectra of ***2*** in different ratios of DMSO/H_2O.

Concentration: 10 μM.

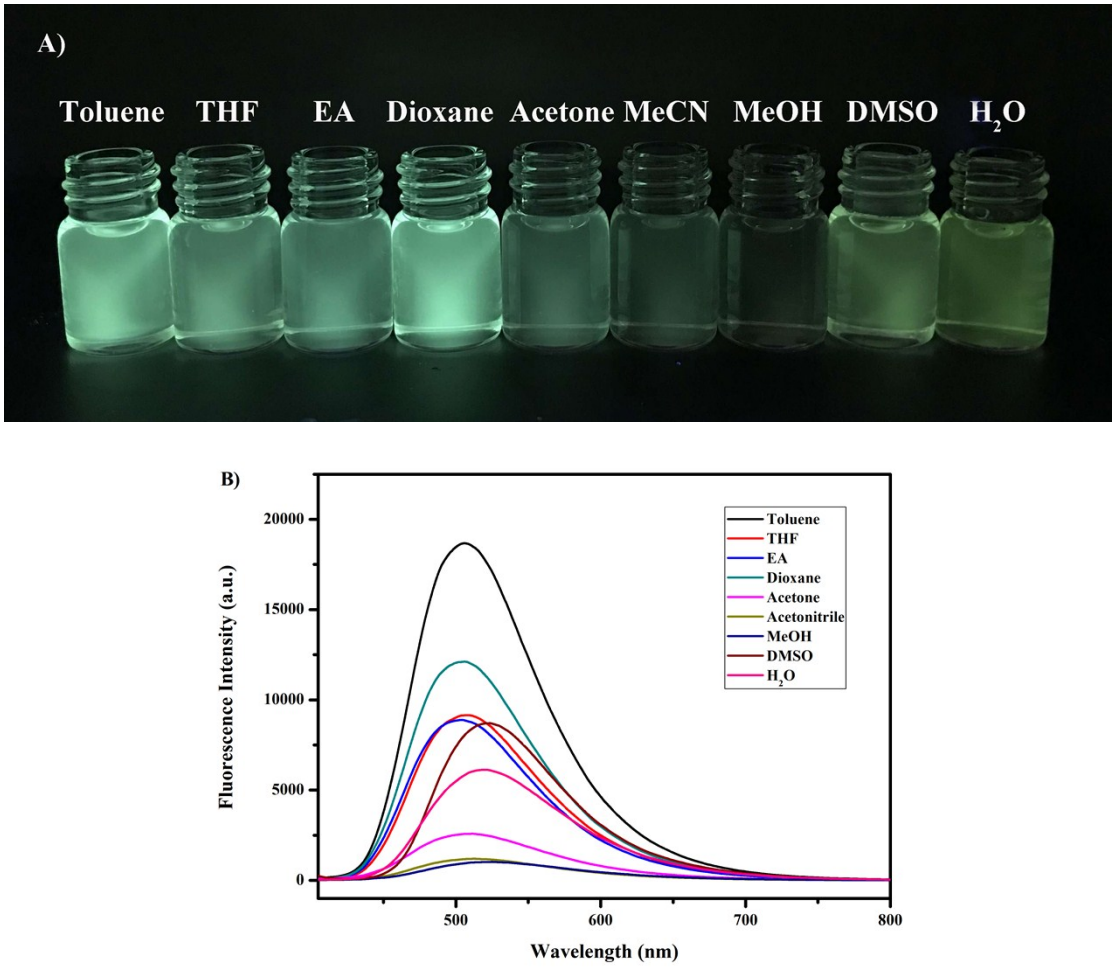

Fig.S12. (A) Fluorescence photography of probe ***2*** in different polar solvents under a UV lamp (365 nm). (B) Fluorescence spectra of probe ***2*** in different solutions. Concentration: 10 μM. Excitation wavelength: 394 nm.

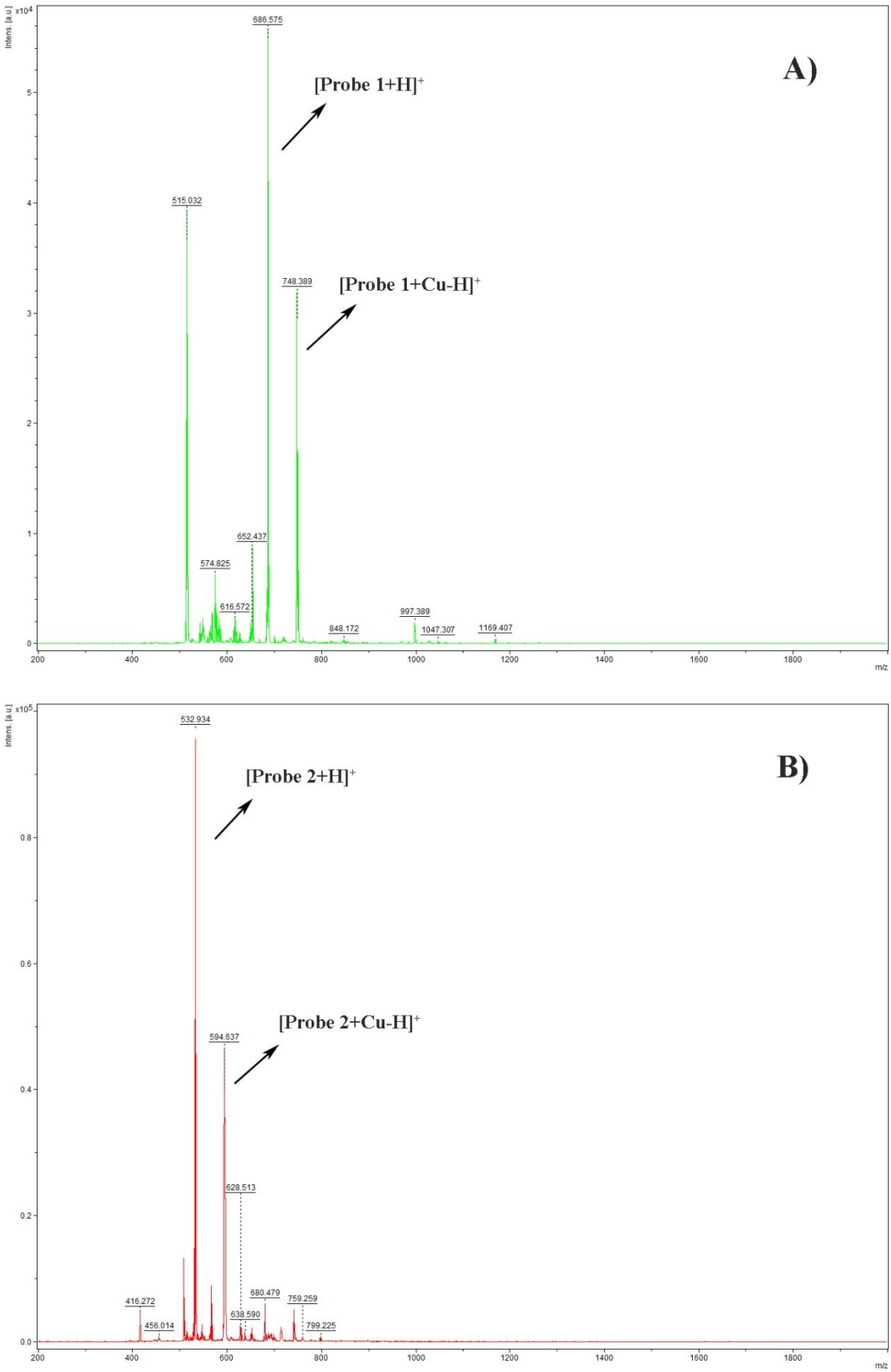

Fig.S13. (A) The MS spectrum of probe ***1*** with Cu^{2+} in CH_3OH. (B) The MS spectrum of probe ***2*** with Cu^{2+} in CH_3OH.

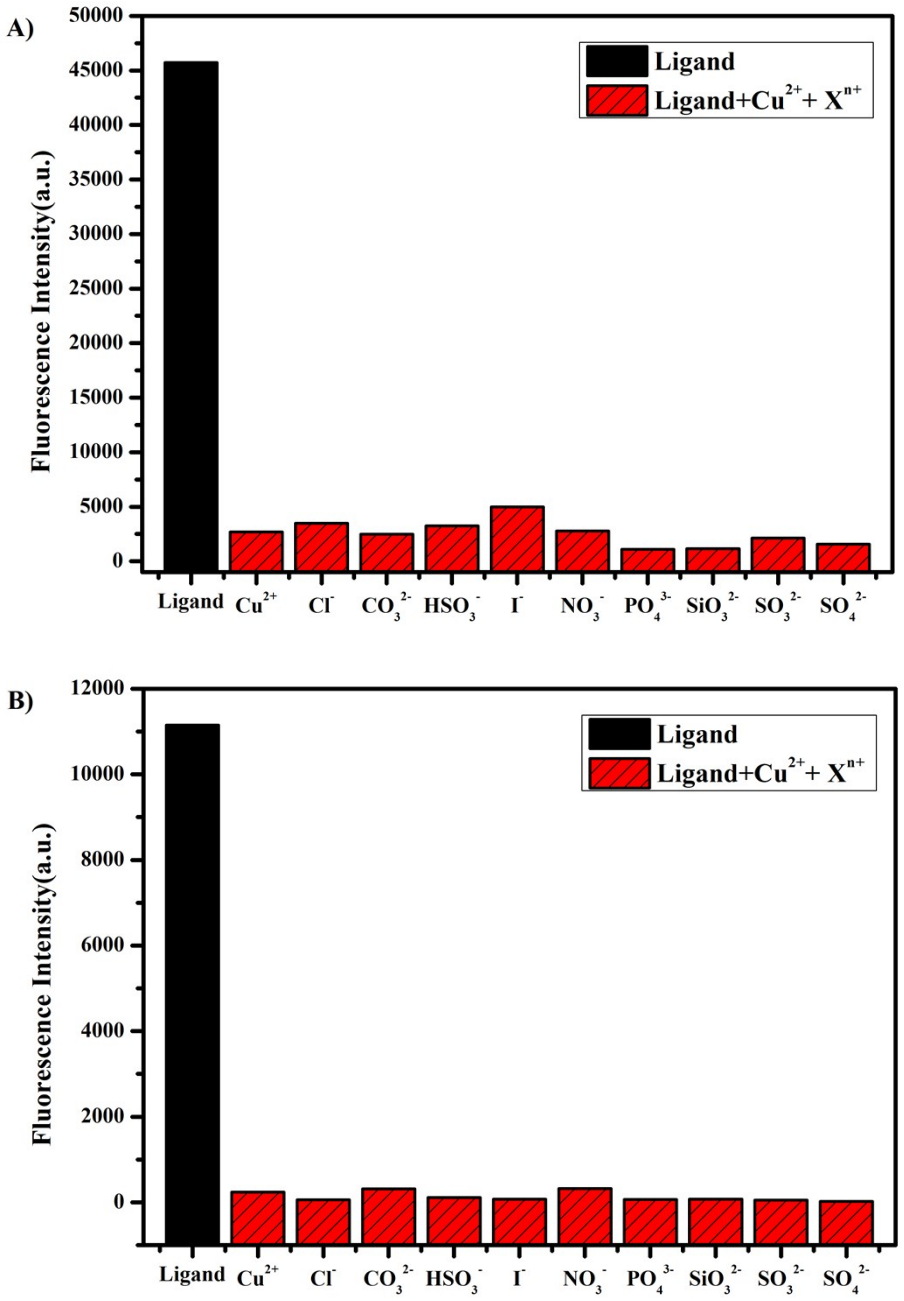

Fig.S14. (A) Fluorescence intensity of probe ***1*** in the presence of 30 μM Cu^{2+} together with 100 μM various coexisting anions. (B) Fluorescence intensity of probe ***2*** in the presence of 15 μM Cu^{2+} together with 100 μM various coexisting anions. Concentration of probe: 10 μM.

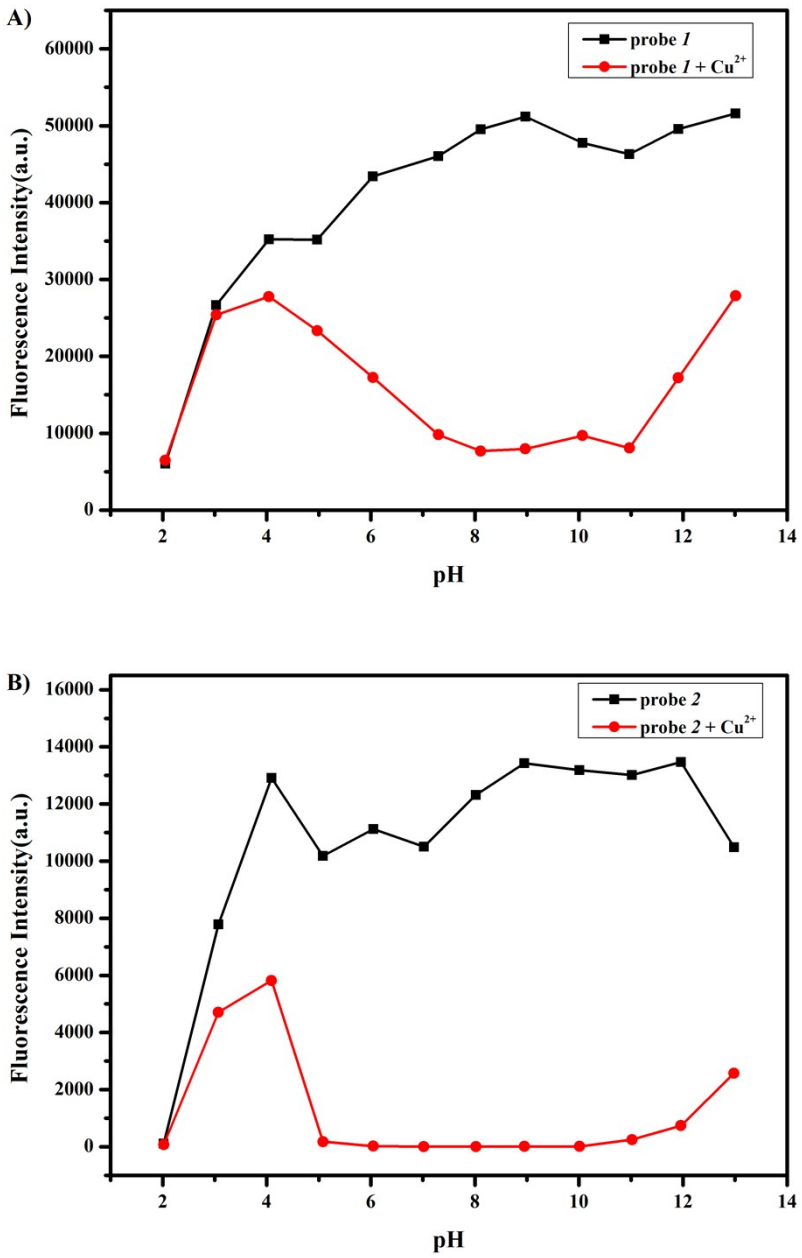

Fig.S15. (A) Fluorescence intensity of probe ***1*** (10 μM) recorded in absence and presence of 30 μM Cu^{2+} at different pHs in DMSO: H_2O (1:1, v/v), λ_{ex}: 370 nm, λ_{em}: 504 nm; (B) Fluorescence intensity of probe ***2*** (10 μM) recorded in absence and presence of 15 μM Cu^{2+} at different pHs in DMSO: H_2O (3:7, v/v), λ_{ex}: 394 nm, λ_{em}: 520 nm.

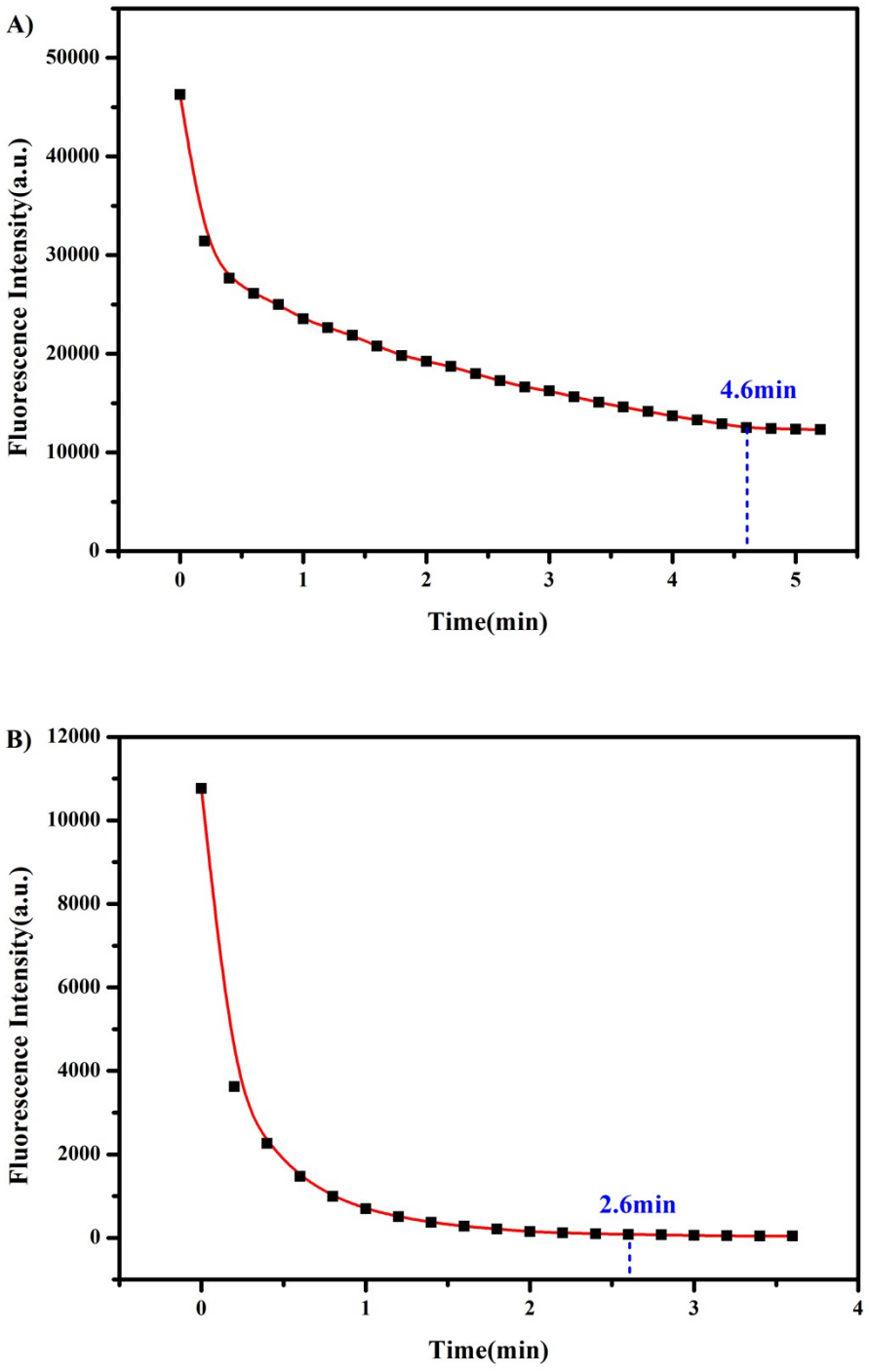

Fig.S16. (A) Time response of probe ***1*** (10 μM) to 3.0 equiv. of Cu^{2+} in DMSO-H_2O (1:1, v/v) solution; (B) Time response of probe ***2*** (10 μM) to 1.5 equiv. of Cu^{2+} in DMSO-H_2O (3:7, v/v) solution.

Table Selected bond lengths (Å), bond angles (°) and torsion angles (°) for probe *1*

Table S1 Bond Lengths for probe *1*.

Atom	Atom	Length/Å	Atom	Atom	Length/Å
O1	C34	1.366(2)	C18	C19	1.377(3)
O1	C38	1.412(2)	C19	C20	1.387(3)
O2	C39	1.220(2)	C21	C22	1.392(3)
N1	C29	1.327(2)	C21	C26	1.392(2)
N1	C33	1.363(2)	C22	C23	1.385(2)
N2	C39	1.343(2)	C23	C24	1.394(2)
N2	C40	1.409(3)	C24	C25	1.399(3)
N3	C47	1.310(2)	C24	C27	1.469(2)
N3	C48	1.366(2)	C25	C26	1.381(2)
C1	C2	1.390(3)	C27	C28	1.329(2)
C1	C6	1.392(3)	C28	C29	1.467(2)
C1	C7	1.492(2)	C29	C30	1.419(3)
C2	C3	1.383(2)	C30	C32	1.355(3)
C3	C4	1.377(3)	C31	C32	1.410(3)
C4	C5	1.380(3)	C31	C33	1.419(3)
C5	C6	1.386(3)	C31	C37	1.417(2)
C7	C8	1.359(2)	C33	C34	1.426(2)
C7	C15	1.487(3)	C34	C35	1.370(2)
C8	C9	1.493(2)	C35	C36	1.407(3)
C8	C21	1.495(2)	C36	C37	1.358(3)
C9	C10	1.396(3)	C38	C39	1.513(3)
C9	C14	1.393(3)	C40	C41	1.374(3)
C10	C11	1.383(3)	C40	C48	1.424(3)
C11	C12	1.387(3)	C41	C42	1.408(3)
C12	C13	1.379(3)	C42	C43	1.356(3)
C13	C14	1.386(3)	C43	C44	1.414(3)
C15	C16	1.387(2)	C44	C45	1.404(3)
C15	C20	1.393(3)	C44	C48	1.415(3)
C16	C17	1.382(3)	C45	C46	1.361(3)
C17	C18	1.379(3)	C46	C47	1.414(3)

Table S2 Bond Angles for probe *1*.

Atom	Atom	Atom	Angle/°	Atom	Atom	Atom	Angle/°
C34	O1	C38	118.37(14)	C25	C24	C27	122.64(16)
C29	N1	C33	117.99(16)	C26	C25	C24	121.40(16)
C39	N2	C40	127.53(16)	C25	C26	C21	120.72(18)
C47	N3	C48	117.41(17)	C28	C27	C24	126.36(18)
C2	C1	C6	118.48(16)	C27	C28	C29	126.55(18)

C2	C1	C7	121.20(17)	N1	C29	C28	115.03(16)
C6	C1	C7	120.24(16)	N1	C29	C30	122.24(16)
C3	C2	C1	120.54(19)	C30	C29	C28	122.72(16)
C4	C3	C2	120.43(19)	C32	C30	C29	119.69(17)
C3	C4	C5	119.83(18)	C32	C31	C33	116.35(16)
C4	C5	C6	119.9(2)	C32	C31	C37	124.30(19)
C5	C6	C1	120.75(19)	C37	C31	C33	119.35(17)
C8	C7	C1	122.71(17)	C30	C32	C31	120.25(18)
C8	C7	C15	122.64(15)	N1	C33	C31	123.44(16)
C15	C7	C1	114.64(14)	N1	C33	C34	117.76(17)
C7	C8	C9	123.15(15)	C31	C33	C34	118.80(16)
C7	C8	C21	120.71(16)	O1	C34	C33	114.31(15)
C9	C8	C21	116.12(14)	O1	C34	C35	125.38(17)
C10	C9	C8	121.26(16)	C35	C34	C33	120.31(18)
C14	C9	C8	120.79(16)	C34	C35	C36	120.01(18)
C14	C9	C10	117.87(17)	C37	C36	C35	121.41(17)
C11	C10	C9	121.25(17)	C36	C37	C31	120.11(19)
C10	C11	C12	120.04(17)	O1	C38	C39	109.84(14)
C13	C12	C11	119.43(18)	O2	C39	N2	126.0(2)
C12	C13	C14	120.53(17)	O2	C39	C38	118.25(17)
C13	C14	C9	120.88(17)	N2	C39	C38	115.73(16)
C16	C15	C7	121.02(16)	N2	C40	C48	116.13(16)
C16	C15	C20	117.80(18)	C41	C40	N2	123.91(18)
C20	C15	C7	121.06(17)	C41	C40	C48	119.93(18)
C17	C16	C15	121.4(2)	C40	C41	C42	119.96(19)
C18	C17	C16	120.2(2)	C43	C42	C41	121.44(19)
C19	C18	C17	119.3(2)	C42	C43	C44	120.1(2)
C18	C19	C20	120.5(2)	C43	C44	C48	119.30(19)
C19	C20	C15	120.8(2)	C45	C44	C43	123.40(19)
C22	C21	C8	120.08(15)	C45	C44	C48	117.29(19)
C22	C21	C26	118.12(16)	C46	C45	C44	119.97(19)
C26	C21	C8	121.73(16)	C45	C46	C47	118.33(19)
C23	C22	C21	121.23(16)	N3	C47	C46	124.22(19)
C22	C23	C24	120.85(17)	N3	C48	C40	118.05(17)
C23	C24	C25	117.66(16)	N3	C48	C44	122.72(17)
C23	C24	C27	119.69(17)	C44	C48	C40	119.21(18)

Table S3 Torsion Angles for probe *1*.

A	B	C	D	Angle/°	A	B	C	D	Angle/°
O1	C34	C35	C36	179.70(17)	C22	C21	C26	C25	1.5(3)
O1	C38	C39	O2	-176.50(17)	C22	C23	C24	C25	-0.7(3)
O1	C38	C39	N2	4.7(2)	C22	C23	C24	C27	177.93(17)
N1	C29	C30	C32	0.1(3)	C23	C24	C25	C26	1.1(3)
N1	C33	C34	O1	1.1(2)	C23	C24	C27	C28	-164.37(19)
N1	C33	C34	C35	-179.19(16)	C24	C25	C26	C21	-1.6(3)
N2	C40	C41	C42	-177.03(18)	C24	C27	C28	C29	179.18(17)
N2	C40	C48	N3	0.1(2)	C25	C24	C27	C28	14.2(3)
N2	C40	C48	C44	178.91(17)	C26	C21	C22	C23	-1.2(3)
C1	C2	C3	C4	-1.6(3)	C27	C24	C25	C26	-177.52(17)
C1	C7	C8	C9	-16.2(3)	C27	C28	C29	N1	-162.72(18)
C1	C7	C8	C21	162.36(16)	C27	C28	C29	C30	17.3(3)
C1	C7	C15	C16	132.92(17)	C28	C29	C30	C32	-179.87(19)
C1	C7	C15	C20	-43.0(2)	C29	N1	C33	C31	2.5(3)
C2	C1	C6	C5	-1.1(3)	C29	N1	C33	C34	-177.63(16)
C2	C1	C7	C8	134.02(19)	C29	C30	C32	C31	1.0(3)
C2	C1	C7	C15	-45.7(2)	C31	C33	C34	O1	-179.06(15)
C2	C3	C4	C5	0.3(3)	C31	C33	C34	C35	0.7(3)
C3	C4	C5	C6	0.5(3)	C32	C31	C33	N1	-1.4(3)
C4	C5	C6	C1	-0.1(3)	C32	C31	C33	C34	178.69(16)
C6	C1	C2	C3	2.0(3)	C32	C31	C37	C36	-179.21(18)
C6	C1	C7	C8	-49.4(3)	C33	N1	C29	C28	178.20(15)
C6	C1	C7	C15	130.89(18)	C33	N1	C29	C30	-1.8(3)
C7	C1	C2	C3	178.62(18)	C33	C31	C32	C30	-0.3(3)
C7	C1	C6	C5	-177.81(18)	C33	C31	C37	C36	0.2(3)
C7	C8	C9	C10	-39.1(3)	C33	C34	C35	C36	0.0(3)
C7	C8	C9	C14	144.29(18)	C34	O1	C38	C39	-169.15(16)
C7	C8	C21	C22	-50.5(2)	C34	C35	C36	C37	-0.6(3)
C7	C8	C21	C26	132.66(19)	C35	C36	C37	C31	0.4(3)
C7	C15	C16	C17	-176.28(17)	C37	C31	C32	C30	179.13(19)
C7	C15	C20	C19	178.09(17)	C37	C31	C33	N1	179.08(17)
C8	C7	C15	C16	-46.8(3)	C37	C31	C33	C34	-0.8(3)
C8	C7	C15	C20	137.28(18)	C38	O1	C34	C33	174.47(15)
C8	C9	C10	C11	-177.94(16)	C38	O1	C34	C35	-5.3(3)
C8	C9	C14	C13	177.14(16)	C39	N2	C40	C41	7.9(3)
C8	C21	C22	C23	-178.13(16)	C39	N2	C40	C48	-170.10(18)
C8	C21	C26	C25	178.44(17)	C40	N2	C39	O2	-6.7(3)
C9	C8	C21	C22	128.17(18)	C40	N2	C39	C38	172.04(17)

C9 C8 C21 C26	-48.7(2)	C40 C41 C42 C43	-1.7(3)
C9 C10 C11 C12	1.2(3)	C41 C40 C48 N3	-178.02(17)
C10 C9 C14 C13	0.4(3)	C41 C40 C48 C44	0.8(3)
C10 C11 C12 C13	-0.4(3)	C41 C42 C43 C44	0.7(3)
C11 C12 C13 C14	-0.4(3)	C42 C43 C44 C45	179.9(2)
C12 C13 C14 C9	0.4(3)	C42 C43 C44 C48	1.0(3)
C14 C9 C10 C11	-1.2(3)	C43 C44 C45 C46	-177.2(2)
C15 C7 C8 C9	163.53(17)	C43 C44 C48 N3	176.97(18)
C15 C7 C8 C21	-17.9(3)	C43 C44 C48 C40	-1.8(3)
C15 C16 C17 C18	-1.8(3)	C44 C45 C46 C47	0.1(3)
C16 C15 C20 C19	2.1(3)	C45 C44 C48 N3	-2.0(3)
C16 C17 C18 C19	2.0(3)	C45 C44 C48 C40	179.29(18)
C17 C18 C19 C20	-0.2(3)	C45 C46 C47 N3	-2.1(3)
C18 C19 C20 C15	-1.8(3)	C47 N3 C48 C40	178.93(17)
C20 C15 C16 C17	-0.3(3)	C47 N3 C48 C44	0.2(3)
C21 C8 C9 C10	142.32(17)	C48 N3 C47 C46	1.9(3)
C21 C8 C9 C14	-34.3(2)	C48 C40 C41 C42	0.9(3)
C21 C22 C23 C24	0.8(3)	C48 C44 C45 C46	1.7(3)

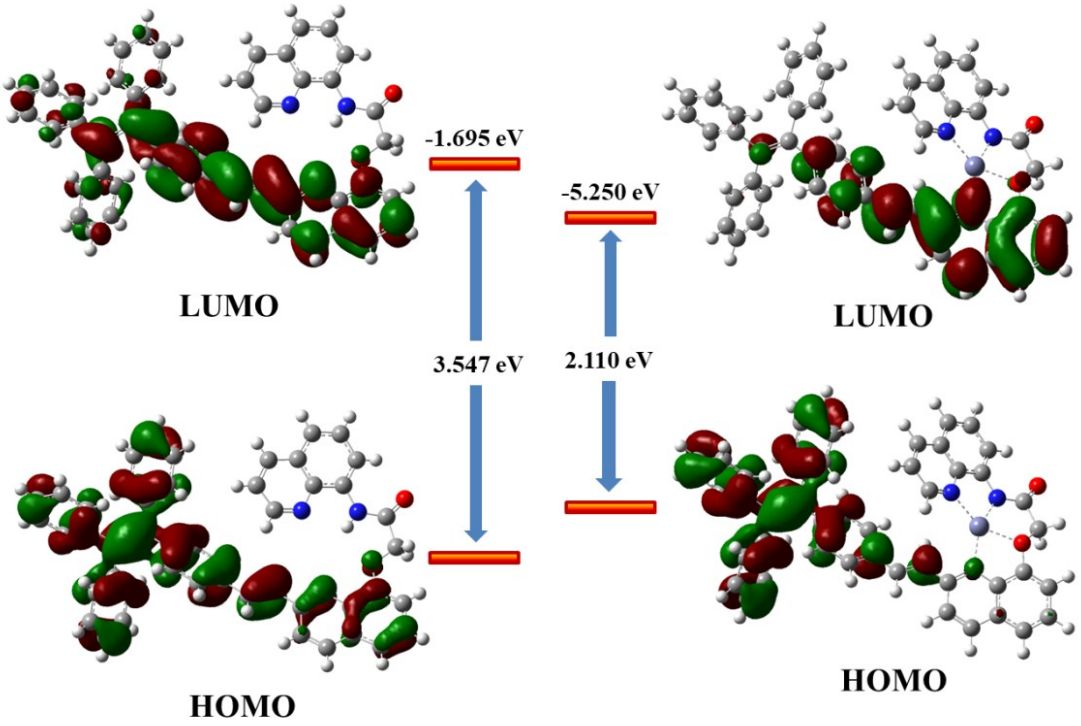

Fig. S17. The frontier molecular orbital distributions and orbital energy levels of free ***1*** and Zn^{2+} adduct complex of ***1.***

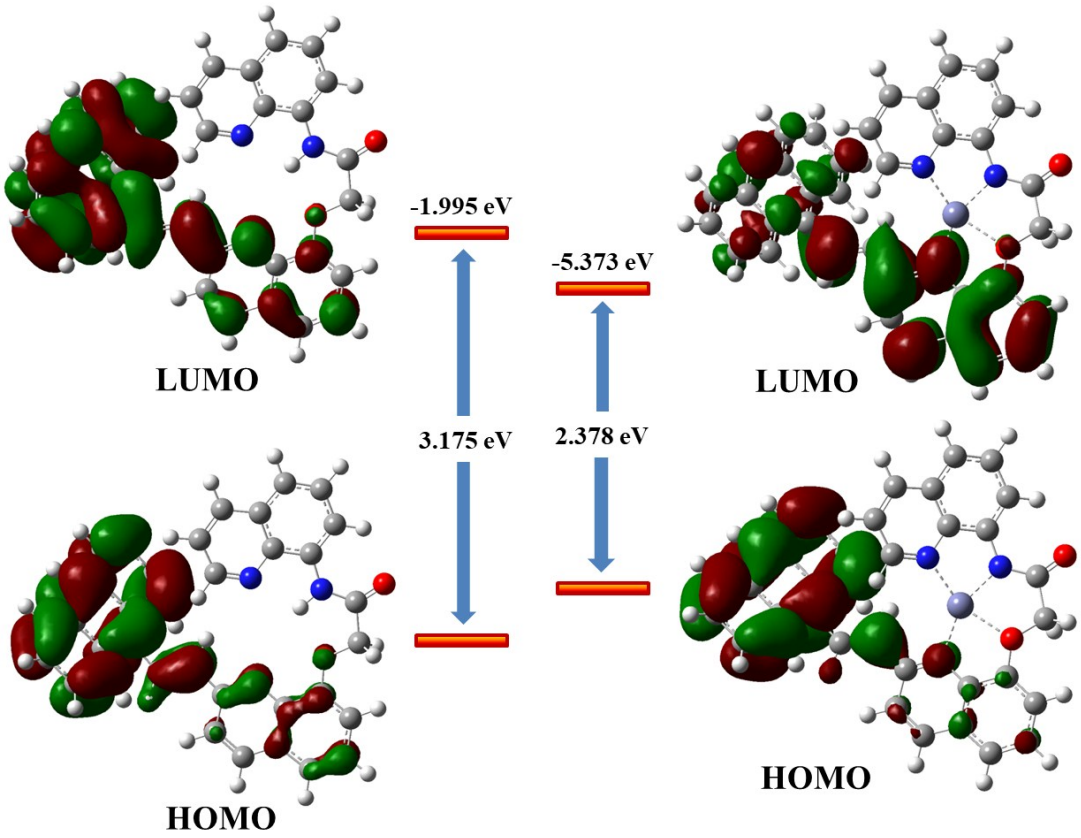

Fig. S18. The frontier molecular orbital distributions and orbital energy levels of free ***2*** and Zn^{2+} adduct complex of ***2***.

Table S4. Selected electronic transition and absorption energies along with their oscillator strengths (f), λ_{abs} of theoretical calculation and experiment of ***1***-Zn^{2+} and ***2***-Zn^{2+}.

Sensors and complexes	Electronic transition	λ_{abs} (nm) (theoretical Values)	λ_{abs} (nm) (experimental Values)	ΔE_{ST} (eV)	f	Excited state
Probe ***1***	$S_0 \rightarrow S_1$	392	370	3.547	0.8285	H to L
1+Zn^{2+}	$S_0 \rightarrow S_1$	668	370	2.110	0.4177	H to L
Probe ***2***	$S_0 \rightarrow S_1$	436	394	3.175	0.3473	H to L
2+Zn^{2+}	$S_0 \rightarrow S_1$	598	394	2.070	0.3016	H to L